An Anti-Aliasing Filter inspired by Continuous-Time ΔΣ Modulation

Pavel Peev[1], Bart De Vuyst[2], Pieter Rombouts[2], and Anas A. Hamoui[1]

[1] Department of Electrical and Computer Engineering, McGill University, Montreal, Canada

[2] Department of Electronics and Information Systems, University of Ghent, Ghent, Belgium

***Abstract* - An anti-aliasing filter that incorporates a sampler is proposed to precede noise-shaping analog-to-digital converters (ADCs), such as discrete-time ΔΣ modulators. The architecture of the proposed anti-aliasing filter is inspired by the implicit anti-aliasing filtering property of CT ΔΣ modulators. However, contrary to CT ΔΣ modulators, the proposed anti-aliasing filter is not sensitive to clock jitter. Furthermore, its key characteristics include: 1) higher suppression of aliases, compared to a Butterworth filter of the same order (same number of opamps); and 2) high-pass shaping of the sampling errors. Its performance advantages are derived theoretically and then confirmed through behavioural simulations.**

I. Introduction

Continuous-time (CT) ΔΣ modulators have recently gained popularity, owing to their potential for low-power high-speed operation, shaping of sampling errors, and implicit anti-aliasing filtering [1]. Discrete-time (DT) ΔΣ modulators are still preferred in many applications, as they do not require tuning circuits nor suffer from clock-jitter sensitivity, compared to CT ΔΣ modulators. However, DT ΔΣ modulators require an explicit anti-aliasing filter. Mixed CT/DT ΔΣ modulators combine the advantages of CT and DT ΔΣ modulators. However, they still suffer from clock jitter, as the DT feedback pulse is subtracted from a CT input signal.

This paper proposes a novel anti-aliasing filter that incorporates a sampler. The filter architecture is inspired by the anti-aliasing filtering characteristics of a CT ΔΣ modulator. However, contrary to CT ΔΣ modulators, it does not suffer from clock-jitter sensitivity. Furthermore, its key features include: 1) higher suppression of aliases, compared to a Butterworth filter of the same order (same number of opamps); and 2) high-pass shaping of the sampling errors (similar to the shaping of quantization noise in a ΔΣ modulator). Thus, the proposed anti-aliasing filter is particularly attractive at the input of DT ΔΣ modulators.

The paper outline is: Section II derives the anti-aliasing property of CT and mixed CT/DT ΔΣ modulators; Section III proposes an anti-aliasing filter with incorporated sampler; and Section IV compares the performance of the proposed anti-aliasing filter to classical filter designs.

II. Anti-Alias Filtering in CT & Mixed ΔΣ Modulators

The implicit anti-aliasing property of CT ΔΣ modulators was first reported in [2], and has since been studied extensively for various modulator architectures [3,4]. This section derives the implicit anti-aliasing property of CT and mixed CT/DT ΔΣ modulators. The equations derived here will then be utilized in Section III to design the proposed anti-aliasing filter.

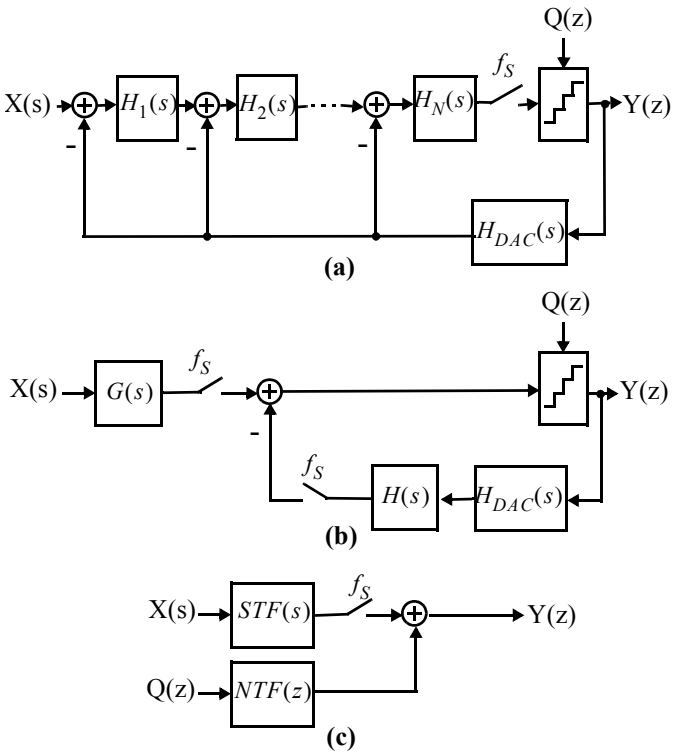

Fig. 1. Block diagram of: **(a)** a CT ΔΣ modulator with distributed DAC feedback; **(b)** the CT ΔΣ modulator in (a), redrawn with loop filter $H(s)$ and input filter $G(s)$; and **(c)** open-loop equivalent representation of the CT ΔΣ modulator in (a).

A. Anti-Aliasing Filtering Characteristics

Consider the linear model of a CT ΔΣ modulator in Fig. 1a. This model can be redrawn as depicted in Fig. 1b, with loop filter $H(s)$ and input filter $G(s)$:

$$G(s) = \prod_{i=1}^{N} H_i(s) \tag{1}$$

$$H(s) = H_N(s) + H_{N-1}(s)H_{N-2}(s) + \ldots + \prod_{i=1}^{N} H_i(s) \tag{2}$$

Define an equivalent DT loop filter:

$$H_{eq}(z) \equiv IIT\{H(s)H_{DAC}(s)\} = Z\left\{ L^{-1}\{H(s)H_{DAC}(s)\}\big|_{t=nT_S} \right\} \tag{3}$$

where $IIT\{.\}$ denotes the impulse invariant transform, while $Z\{.\}$ and $L\{.\}$ denote the Z-transform and the Laplace transform, respectively.

978-1-4244-2182-4/08/$25.00 ©2008 IEEE.

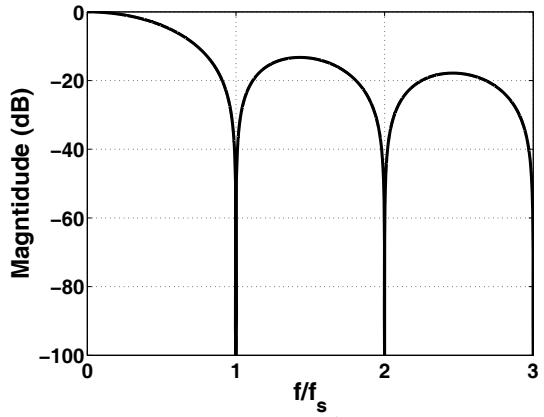

Fig. 2. Magnitude response of STF for a 1st-order CT ΔΣ modulator. Observe the notches at multiples of f_S.

Then, the output of the CT ΔΣ modulator (Fig. 1b) can be expressed as:

$$Y(z) = \frac{[G(s)X(s)]^*}{1+H_{eq}(z)} + \frac{Q(z)}{1+H_{eq}(z)} \tag{4}$$

where * denotes the sampling operation, as in [5]. Thus, the noise transfer function (from $Q(z)$ to $Y(z)$) is given by:

$$NTF(z) \equiv \left.\frac{Y(z)}{Q(z)}\right|_{X(s)=0} = \frac{1}{1+H_{eq}(z)} \tag{5}$$

Hence, using (4) and (5), the ΔΣ modulator output can be expressed as:

$$Y(z) = [G(s)X(s)]^* NTF(z) + NTF(z)Q(z) \tag{6}$$

The NTF in (6) can now be inserted in the sample operation by setting $z = e^{sT_S}$, thereby resulting in:

$$Y(z) = [G(s)NTF(e^{sT_S})X(s)]^* + NTF(z)Q(z) \tag{7}$$

where $T_S = 1/f_S$ is the clock sampling period.

Accordingly, to represent the CT ΔΣ modulator in Fig. 1b, the open-loop equivalent model in Fig. 1c can be utilized. Here, the signal-transfer function (STF) prior to the sampling operation is defined as:

$$STF(s) \equiv \left.\frac{Y(e^{sT_S})}{X(s)}\right|_{Q(z)=0} = G(s)NTF(e^{sT_S}) = \frac{G(s)}{1+H_{eq}(e^{sT_S})} \tag{8}$$

To illustrate how the STF in equation (8) results in anti-aliasing filtering, consider for example a 1st-order CT ΔΣ modulator with:

$$H(s) = G(s) = \frac{1}{sT_S} \tag{9}$$

$$H_{DAC}(s) = \frac{1-e^{-sT_S}}{s} \tag{10}$$

where the loop filter $H(s)$ is a CT integrator and the feedback pulse shaper (i.e., the digital-to-analog converter (DAC)) is a zero-order hold.

Figure 2 plots the magnitude response of the STF in equation (8), after substituting (9) and (10) into (8). Observe that the STF has notches at multiples of f_S, where $f_S = 1/T_S$ is the sampling frequency.

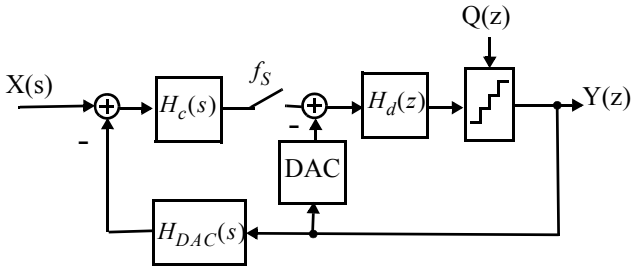

Fig. 3. Block diagram of a mixed CT/DT ΔΣ modulator.

Signals aliasing into the input-signal band are found in the frequency range $kf_S \pm f_{BW}$, where f_{BW} is the input-signal band edge and k is an integer. The oversampling ratio is defined as:

$$OSR = \frac{f_S}{2f_{BW}} \tag{11}$$

Since, typically $OSR \gg 1$, the inband aliasing signals fall close to the notches of the STF. Therefore, these signals are suppressed before they are aliased inband by the sampling operation. Furthermore, as the OSR increases, the inband aliasing signals occur closer to the STF notches and, hence, the amount of suppression increases.

B. Anti-Aliasing Filtering in Mixed CT/DT ΔΣ Modulators

Mixed CT/DT ΔΣ modulators combine CT integrators and DT integrators, as shown in Fig. 3 [6, 7]. An analysis of the output yields:

$$Y(z) = \frac{[H_c(s)X(s)]^* H_d(z) + Q(z)}{1 + H_{c,eq}(z)H_d(z) + H_d(z)} \tag{12}$$

Here, $H_{c,eq}(z)$ is the equivalent discrete-time filter of $H_c(s)$ as defined in (3). Thus, the STF prior to the sampling operation (as depicted in Fig. 1c) is given by:

$$STF(s) = \frac{H_c(s)H_d(e^{sT_S})}{1 + H_{c,eq}(e^{sT_S})H_d(e^{sT_S}) + H_d(e^{sT_S})} \tag{13}$$

Observe that for frequencies near multiples of f_S, the STF in (13) reduces to:

$$STF(s)|_{f \to kf_S} = \frac{H_c(s)}{1 + H_{c,eq}(e^{sT_S})} \tag{14}$$

Accordingly, based on (14), the amount of anti-aliasing suppression in a mixed ΔΣ modulator (Fig. 3) depends solely on the order of its continuous-time filter $H_c(s)$.

III. Proposed Anti-Aliasing Filter

A. Proposed Filter Architecture

To design an anti-aliasing filter, this paper proposes using a CT ΔΣ modulator without a quantizer, as depicted in Fig. 4a. Here, a zero-order hold (ZOH)

$$ZOH(s) = \frac{1-e^{-sT_S}}{s} \tag{15}$$

is used to implement the feedback pulse shaper.

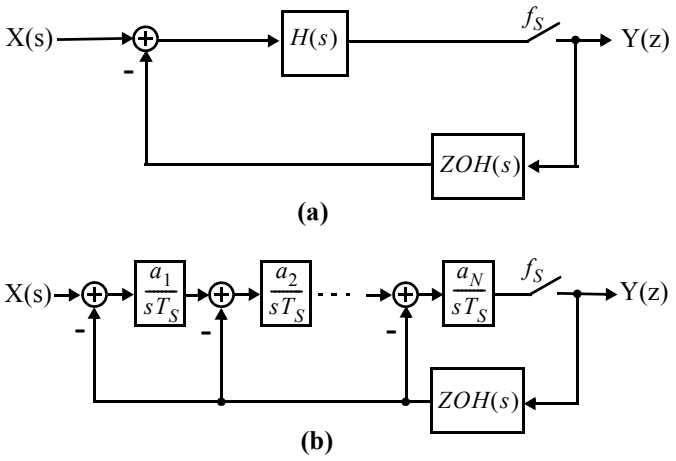

Fig. 4. Proposed anti-aliasing filter with incorporated sampler: **(a)** generic representation; and **(b)** proposed implementation.

The proposed anti-aliasing filter (Fig. 4a) does not suffer from clock jitter sensitivity (compared to classical CT ΔΣ modulators), since it has no quantizer. Furthermore, since the sampler is incorporated inside the loop, sampling errors are high-pass shaped (similar to the shaping of quantization noise in a ΔΣ modulator). However, the trade-off is that a sample-and-hold circuit is needed to implement the sampler. Accordingly, the proposed anti-aliasing filter is particularly attractive at the input of noise-shaping ADCs, such as DT ΔΣ modulators.

B. Proposed Filter Implementation

To implement the proposed anti-aliasing filter architecture (Fig. 4a), the *N*-th order feedback filter in Fig. 4b is proposed. Here, a distributed feedback (rather than feedforward) architecture is selected, as it results in an equivalent forward filter $G(s)$ with only poles and, hence, it maximizes the achievable anti-aliasing suppression.

The proposed anti-aliasing filter in Fig. 4b can be mapped to Fig. 1b, with:

$$G(s) = \frac{\prod_{i=1}^{N} a_i}{(sT_S)^N} \tag{16}$$

$$H(s) = \frac{a_N}{sT_S} + \frac{a_N a_{N-1}}{(sT_S)^2} + \ldots + \frac{\prod_{i=1}^{N} a_i}{(sT_S)^N} \tag{17}$$

Since the derivation of the anti-aliasing property of CT ΔΣ modulators in Section II involved setting $Q(z) = 0$, the exact analysis is applicable to the proposed anti-aliasing filter in Fig. 4b. Accordingly, based on equation (8), the transfer function from input $X(s)$ to output $Y(e^{sT_S})$ *before* the sampler in the proposed anti-aliasing filter (Fig. 4b) can be expressed as:

$$F_{AA}(s) \equiv \frac{Y(e^{sT_S})}{X(s)} = G(s)NTF(e^{sT_S}) \tag{18}$$

where $NTF(e^{sT_S})$ is given in (5).

Owing to the chain of integrators, the loop filter $H(s)$ in (17) has an equivalent discrete-time filter $H_{eq}(z)$ in (3) with all its poles at $z = 1$ (dc) and with the location of its zeros dependent on the coefficients a_i. Therefore, the corresponding NTF in (5) can be expressed as:

$$NTF(z) = \frac{(z-1)^N}{\prod_{p=1}^{N}(z-z_p)} \tag{19}$$

where the location of poles z_p depends on coefficients a_i. Thus, $NTF(z)$ has a high-pass characteristic with notches at multiples of f_S.

C. Minimum Aliasing Suppression

The signals aliasing into the input-signal band are found in the frequency range $kf_S \pm f_{BW}$ $(k = 1, 2, \ldots)$. Therefore, since the anti-aliasing filter is a low-pass filter, the signals at $f = f_S - f_{BW}$ are the least suppressed. Hence, the inverse magnitude response of the anti-aliasing filter at $f = f_S - f_{BW}$ (i.e., $1/|F_{AA}(f_S - f_{BW})|$) corresponds to the worst-case suppression of the aliases by the anti-aliasing filter. This is referred to as the *minimum aliasing suppression*.

Accordingly, substituting (16) and (19) in (20), the minimum aliasing suppression can be expressed as:

$$\frac{1}{|F_{AA}(f_S - f_{BW})|} = \frac{|j2\pi(f_S - f_{BW})T_S|^N}{\prod_{i=1}^{N} a_i} \cdot \frac{\prod_{p=1}^{N} |e^{j2\pi(f_S - f_{BW})T_S} - z_p|}{|e^{j2\pi(f_S - f_{BW})T_S} - 1|^N} \tag{20}$$

To simplify (20), observe that:

1) For $OSR \gg 1$:
$$e^{j2\pi(f_S - f_{BW})T_S} = e^{-j\frac{\pi}{OSR}} \approx 1 \tag{21}$$

2) At low frequencies, the STF of a CT ΔΣ modulator and, equivalently, the magnitude response of $F_{AA}(s)$ in (18) are approximately unity. This results in:
$$\lim_{f \to 0} |F_{AA}(f)| = \lim_{f \to 0} \left| \frac{G(j2\pi f)}{1 + H_{eq}(e^{j2\pi f T_S})} \right| = 1 \tag{22}$$
Substituting (16) and (19) into (22), results in:
$$\prod_{i=1}^{N} a_i = \prod_{p=1}^{N} |1 - z_p| \tag{23}$$

Using (21) and (23), equation (22) can be simplified as:

$$\frac{1}{|F_{AA}(j2\pi(f_S - f_{BW}))|} = \frac{|e^{-j\frac{\pi}{OSR}} - 1|^N}{|j2\pi(f_S - f_{BW})T_S|^N} \tag{24}$$

Using Euler's formula, some trigonometric identities, and Taylor's expansion, equation (24) can be further simplified to express the minimum aliasing suppression as:

$$\frac{1}{|F_{AA}(f_S - f_{BW})|} = (2OSR)^N \tag{25}$$

This result demonstrates that the minimum aliasing suppression of the proposed anti-aliasing filter is only dependent on the OSR and the filter order *N*.

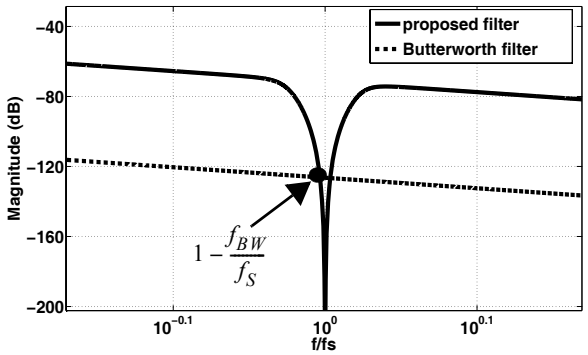

Fig. 5. Magnitude response of the proposed anti-aliasing filter and a low-pass Butterworth with 3-dB cutoff at the signal-band edge f_{BW}. Observe that both responses intersect at $f = f_S - f_{BW}$ ($N = 3$, $OSR = 64$).

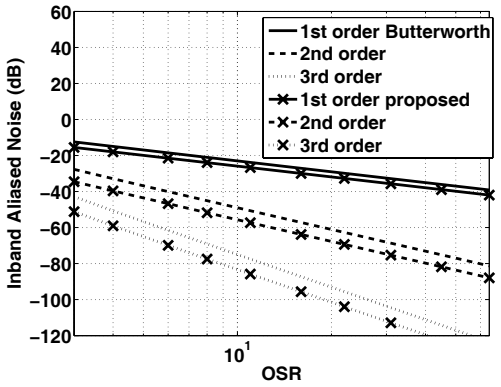

Fig. 6. Inband alias power P_{alias} versus oversampling ratio OSR, using the proposed anti-aliasing filter and a low-pass Butterworth filter, for various filter orders.

IV. Performance Comparison to Butterworth Filters

A. Minimum Aliasing Suppression

Consider a classical N^{th}-order low-pass Butterworth filter with 3-dB corner frequency at the signal-band edge f_{BW}. Its transfer function is given by:

$$F_{\text{BUTTER}}(f) = \frac{1}{\sqrt{1+\left(\frac{f}{f_{BW}}\right)^{2N}}} \tag{26}$$

When used as an anti-aliasing filter, this Butterworth filter has minimum aliasing suppression of:

$$\frac{1}{|F_{\text{BUTTER}}(f_S - f_{BW})|} \approx (2OSR)^N \tag{27}$$

Comparing (27) and (25) reveals that the proposed anti-aliasing filter has a minimum suppression equivalent to a classical Butterworth filter of the same order. This is shown graphically in Fig. 5, where the magnitude responses of the proposed and Butterworth anti-aliasing filters are plotted.

B. Inband Alias Power

Another way to compare the performance of anti-aliasing filters is to calculate the total signal power at the filter output that can alias into the signal band, assuming a normalized signal with a white spectrum at the filter input. This is referred to as the inband alias power P_{alias}. Since signals in the frequency range $kf_S \pm f_{BW}$ ($k = 1, 2, \ldots$) can alias inband, the alias power is given by

$$P_{\text{alias}} = \frac{1}{f_{BW}} \sum_{k=1}^{\infty} \int_{(kf_S - f_{BW})}^{(kf_S + f_{BW})} |F(f)|^2 \, df \tag{28}$$

where $|F(f)|$ is the magnitude response of the filter.

Intuitively, less aliasing (smaller P_{alias}) is expected using the proposed anti-aliasing filter, since it has notches at multiples of f_S. Figure 6 compares the aliasing power P_{alias} of the proposed anti-aliasing filter and a low-pass Butterworth filter for various filter orders. In this figure, P_{alias} was computed over only the first 10 inband-aliasing frequency ranges (i.e., for k=1,..., 10 in equation (28)), as alias signals at frequencies above these ranges are highly suppressed and, hence, are insignificant.

As per Fig. 6, for a given filter order, the proposed anti-aliasing filter achieves more noise power suppression (smaller P_{alias}) than a Butterworth filter. Furthermore, as the filter order increases, the performance of the proposed filter improves compared to a Butterworth filter. Accordingly, the aliasing suppression advantages of the proposed anti-aliasing filter are most noticeable when designed for higher orders, where it would significantly outperform a Butterworth filter.

V. Conclusion

A novel anti-aliasing filter that incorporates a sampler has been proposed. Compared to a Butterworth filter of the same order, the proposed filter has the same minimal alias suppression. Furthermore, it has higher overall alias suppression, owing to the notches in the magnitude response at multiples of the sampling frequency. This anti-aliasing performance advantage of the proposed filter increases as the filter order increases. In addition, the proposed filter high-pass shapes the sampling errors (similar to the shaping of quantization noise in ΔΣ modulators). Accordingly, the proposed anti-aliasing filter is particularly attractive at the input of oversampling discrete-time ΔΣ modulators.

VI. References

[1] P. M. Chopp, and A. A. Hamoui, "Discrete-Time Modeling of Clock Jitter in Continuous-Time ΣΔ Modulators" in *Proc. IEEE Int. Symp. Circuits Syst.*, pp. 497-300, May 2007.

[2] J. C. Candy, "A Use of Double Intergration in Sigma Delta Modulation," *IEEE Transactions on Communications*, vol. 3, no. 3, March 1985.

[3] M. Keller, A. Buhmann, M. Ortmanns, and Y. Manoli, "On the Implicit Anti-Aliasing Feature of Continuous-Time Multistage Noise-Shaping Sigma-Delta Modulators," in *Proc. IEEE Int. Symp. Circuits Syst.*, pp. 721-724, May 2007.

[4] O. Shoaei and W. M. Snelgrove, "Design and Implementation of a Tunable 40 MHz-70 MHz Gm-C Bandpass ΔΣ Modulator," *IEEE Trans. Circuits Syst. II*, vol. 44, no. 7, pp. 521-530, July 1997.

[5] J. De Maeyer, P. Rombouts, and L. Weyten, "Efficient Multibit Quantization in Continuous-Time ΔΣ Modulators," *IEEE Trans. Circuits Syst.-I*, vol. 54, pp. 757-767, Apr. 2007.

[6] K. Nguyen *et al*., "A 106dB SNR Hybrid Oversampling Analog-to-Digital Converter for Digital Audio," *IEEE J. Solid-State Circuits*, vol. 40, no. 12, pp. 2408-2415, December 2005.

[7] B. Putter, "A 5th-order CT/DT Multi-Mode ΔΣ Modulator," *IEEE Solid-State Circuits Conf.*, pp 244-245, Feb. 2007.

[8] M. Ortmanns, F. Gerfers, and Y. Manoli, "A Continuous-Time Sigma-Delta Modulator with Switched Capacitor Current Mode Feedback", in *Proc. European Solid-State Circuits Conf.,* pp. 249-252, Sept. 2003.